Author/s:
Chakraborty, S;Xu, Y;Roberts, A;Goswami, D;Smith, TA

Title:
An investigation of evanescent wave-induced fluorescence spectroscopy for exploring high refractive index media

Date:
2023-01-01

Citation:
Chakraborty, S., Xu, Y., Roberts, A., Goswami, D. & Smith, T. A. (2023). An investigation of evanescent wave-induced fluorescence spectroscopy for exploring high refractive index media. Physica Scripta, 98 (1), https://doi.org/10.1088/1402-4896/aca437.

Persistent Link:
https://hdl.handle.net/11343/333152

An investigation of Evanescent Wave-Induced Fluorescence Spectroscopy for Exploring High Refractive Index Media

An investigation of Evanescent Wave-Induced Fluorescence Spectroscopy for Exploring High Refractive Index Media

Subhajit Chakraborty,[1,2,3,6] Yang Xu,[2,3] Ann Roberts,[3,4,5] Debabrata Goswami[1,6,*] and Trevor A. Smith[2,3,#]

[1] *Centre for Lasers & Photonics, IIT Kanpur, Kanpur, India*

[2] *School of Chemistry, University of Melbourne, Victoria, 3010, Australia*

[3] *ARC Centre of Excellence in Exciton Science, School of Chemistry, University of Melbourne, Victoria, 3010, Australia*

[4] *School of Physics, University of Melbourne, Victoria, 3010, Australia*

[5] *ARC Centre of Excellence for Transformative Meta-Optical Systems, School of Physics, University of Melbourne, Victoria, 3010, Australia*

[6] *Department of Chemistry, IIT Kanpur, Kanpur, India*

** dgoswami@iitk.ac.in*

 # trevoras@unimelb.edu.au

Abstract:

Evanescent wave-induced fluorescence spectroscopy (EWIFS) is a widely used technique for probing the interfacial behavior of different complex media in investigations of samples in the physical, chemical, and biological sciences. This technique takes advantage of the sharply decaying evanescent field, established following total internal reflection (TIR) at the interface of two media, for spatially identifying the photoluminescence characteristics of the sample. The generation of the evanescent field requires the refractive index of the second medium to be lower than that of the first, so a major disadvantage of this increasingly widely used spectroscopic technique is the inability to exploit the advantages of EWIFS to image a sample with a higher refractive index than the incident substrate medium. A proposed configuration in which a thin, low refractive index intermediate layer is established between the TIR substrate and a high refractive index sample is investigated. We illustrate that this arrangement does not afford the desired advantages of evanescent field-induced fluorescence measurements for investigating high refractive index media.

Introduction:

Evanescent field-induced fluorescence is a near-field optical spectroscopic and microscopic tool based on total internal reflection that is widely used in biochemistry, cell biology and biophysical applications[1]. It is also of importance in many areas of materials science{Simpson, 1997 #48;Woerdeman, 1996 #49}. When an electromagnetic (EM) field is incident at an interface of two media of different refractive indices, a component of the EM wave is reflected into the first medium, and the rest is transmitted into the second medium. The proportions of the reflected and transmitted parts are governed by Fresnel's equations[4]. When the refractive index of the second medium is higher than that of the first medium, the amount of the incident wave being transmitted to the second medium is a function of the incident angle of the EM wave at the interface. When the refractive index of the second medium is less than that of the first, the incident beam is totally reflected from the interface if the incidence angle exceeds the critical angle; producing the phenomenon known as the total internal reflection (TIR)[5]. Under such conditions, an evanescent field is generated within the second medium as a result of the TIR at the interface, and this field strength decays exponentially with distance (typically, within some hundreds of nanometers) from the interface. The penetration depth of the evanescent field, d_p, is defined as the distance, normal to the interfacial plane, required for the electric field amplitude to fall to 1/e of its initial value at the interface. This distance d_p is a function of the incident angle, θ_i, the wavelength of light used, λ, and the relative refractive indices of the two media, n_1 and n_2:

$$d_p = \frac{\lambda}{2\pi} \frac{1}{\sqrt{n_1^2 \theta_i - n_2^2}} \quad (1)$$

approaching infinity when θ_i is close to the critical angle defined by Snell's law ($\theta_c = \sin^{-1}\left(\frac{n_2}{n_1}\right)$ assuming $n_2 < n_1$). It should be noted that the penetration depth is often also defined by the electric field intensity, i.e. $I = I_0 e^{\frac{-z}{\Lambda}}$, where I and I_0 are intensities in the optically rarer medium and at the

interface, respectively. In this case, Λ is half the value of d_p. Chromophores within the region of the lower refractive index medium into which the evanescent wave extends can absorb energy from the field and become photoexcited leading to attenuation of the "totally internally" reflected beam. Absorption spectral information can be extracted through measurements of the wavelength-dependent attenuation of the reflected beam, usually in a multiple bounce geometry to enhance the attenuation and thereby signal-to-noise[6].

If the photoexcited chromophores are fluorescent, their emission can be used to probe photophysical behavior in a region in close proximity of the interface, in the technique known as evanescent wave-induced fluorescence spectroscopy (EWIFS)[7] or total internal reflection fluorescence (TIRF)[8]. The sensitivity of fluorescence techniques along with the inherent spectral and temporal information, make this an attractive approach to probe variations in the photophysical behavior with distance from the interface. This approach can be further extended to the microscopic regime; total internal reflection fluorescence microscopy (TIRFM)[9]. In TIRFM the excitation of fluorophores near the interface results in high contrast images containing spectral (and temporal) information near the interface. The main advantage of this technique is the selective photoexcitation of, and therefore emission from, the surface bound fluorophores where the molecules residing deep inside the sample volume are not excited and hence, cannot emit. The sub-micron surface selectivity has led to this technique becoming a common choice for high resolution imaging at the single molecule level[10] and in some implementations of structured illumination microscopy[11,12].

TIR-based techniques offer some significant advantages over other methods. One common implementation of EW spectroscopy is to probe a signal (absorption or emission) as a function of distance from the interface by varying d_p through changing the angle of incidence (variable angle EW spectroscopy)[5,6]. In addition, the potential to probe molecular alignment and dynamics (in- and out-of- the plane of the substrate) through exploiting the polarization properties of the evanescent field (to preferentially excite absorption transition moments oriented either in either in- and out-of- the plane

of the substrate surface using *s*- or *p*-polarised excitation, respectively)[13] is attractive for many fields beyond a biological context, including materials chemistry[14].

In a conventional evanescent wave experiment, the first medium (TIR substrate) is generally taken as a glass (e.g. silica, SiO_2), although such measurements can also be performed at the interface between two liquids,[15] a plasma and a liquid[16] or a liquid and a gas.[17] Evanescent wave excitation of the object is possible while the refractive index, n, of the sample does not exceed that of the glass (n = 1.47 at 400 nm for silica[18]). The major disadvantage of EW techniques arises when the refractive index of the sample of interest is higher than that of the first (substrate) medium, whereby TIR does not occur, and the evanescent field cannot be generated from the interface of the two media. A solution in some cases is to use a material of refractive index higher than common glass, for example sapphire (alumina, Al_2O_3, n=1.79 at 400 nm[19]), $LaSFO_8$[20] (n=1.92 at 400 nm[21]) or TiO_2,[22] (n=2.87 at 400 nm[23]) or $SrTiO_3$[22] (n=2.5803 at 400 nm[24]) as the incident substrate material. For practical applications in fields such as materials science, many sample materials of interest, including films of organic polymers and perovskites, have very high refractive indices (sometimes exceeding 2). Therefore, utilizing the advantages of evanescent field induced fluorescence measurements is generally not possible for films of these materials on regular prism substrates by the conventional EW-based approach.

In order to overcome this issue, we investigate an arrangement where the evanescent field induced emission mode may become possible even for objects having refractive index higher than the first medium. In this system a very thin film of a material with refractive index less than that of the first medium is sandwiched between the first medium and the object. A schematic diagram of the arrangement is shown in Figure 1.

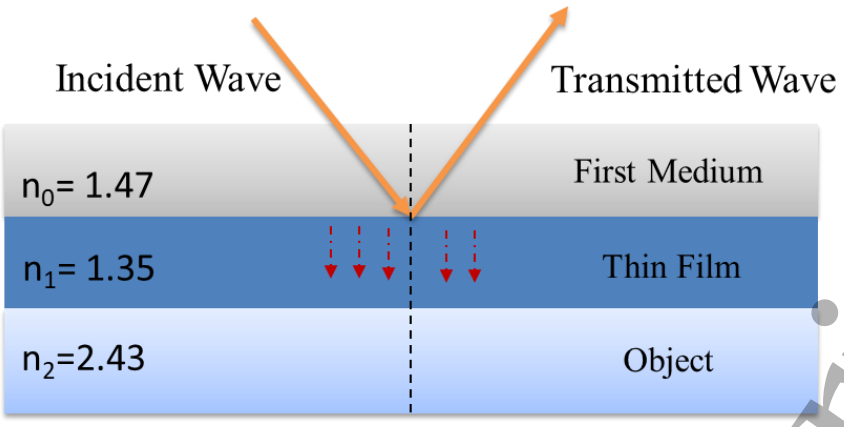

FIG. 1. Schematic diagram of the layered TIR arrangement

When the angle of incidence of the light at the n_0 : n_1 interface exceeds the critical angle for the n_0 and n_1 materials, total internal reflection of the incident EM wave can occur within the n_0 material and an EW may be generated in the n_1 material, given certain constraints. The evanescent field thereby generated in the n_1 film loses its strength, generally within some hundreds of nanometers from the n_0 : n_1 interface. If the thickness of the n_1 film is large enough so that coupling across the gap is very weak, the evanescent field will decay within the thin film itself and never reach the n_2 material – the third layer is essentially irrelevant. It is tempting to consider that if the intermediate (n_2) layer is made very thin then any EW generated at the n_0:n_1 interface may have a possibility of transmitting through the thin n_1 layer and into the third (n_2) medium. The evanescent field could then excite the fluorophores in n_2 within proximity of the n_1 : n_2 interface and the emission from these molecules can be captured with a sensitive detector. On the other hand, a very thin film of the n_1 material may not constitute a true low refractive index medium relative to n_0 and no evanescent wave will be established.

Multilayer systems have previously been reported by several other researchers. A similar three-layer system based on a prism-air-fiber arrangement is reported by Saloman et al.[25]. In their setup, a beam was incident into a glass prism (n=1.458) and was totally reflected with angle of incidence larger than the critical angle. A fiber tip was put on the evanescent wave side of the prism with a gap, which was changed to probe the intensity of the evanescent field as a function of distance to the surface. They found that while probing with a fiber tip, the evanescent field being detected didn't drop exponentially,

which proves that the fiber affects the generated field, especially when the fiber is close to the prism. Other systems based on prism-air-substrate layers have been implemented to achieve frustrated TIR[26,27]. Harrick[5] reported a prism-air-prism system where two prisms were placed very close to each other but without contact. It was found that when the distance between the two prisms is a fraction of the incident wavelength, the reflected beam will be attenuated. The transmitted intensity was found to increase as the distance between two prisms decreases indicating that the incident light is coupled into the second prism medium.

Multi-layered approaches exploiting resonant enhancement of evanescent waves have been invoked to increase the evanescent field strength for applications such as atomic mirrors[28] and optical trapping, using graphene and double-negative materials.[29,30] A related approach is exploited in surface plasmon resonance experiments[31,32] in which a thin film of metal (e.g. Au or Ag) is coated onto a typical (silica) substrate. Thin films of such metals have a very low refractive index, e.g. thin films of Ag have n=0.06422[33] (0.056[34]) at 400 nm. When the electrical field energy of the photon matches the optical properties dictated by the thickness of the metal layer, it can interact with the free electron oscillations in the metal film; these are the outer shell and conduction-band electrons. The incident photons are absorbed, and the energy is transferred to the electrons, which convert into surface plasmons. A surface plasmon is established that can enhance the field strength at the interface and create an evanescent field that extends into the medium on either side of the film that decays rapidly with distance from the interface. The plasmon is generated with *p*-polarized light. Surface plasmons can also be used to induce emission in the interfacial region (surface plasmon-coupled emission).[35] Rather than providing an inert, low refractive index layer, the materials employed for these resonance-based multi-layer systems may also influence the photophysical properties, including fluorescence quantum yield/lifetime, which is undesired in the experiments under consideration in this paper.

Indeed, there have been previous attempts to perform EW spectroscopy to study films of high refractive index materials using such an approach. For example, in a study of perovskite materials,[36,37] a low

refractive index layer (an air gap only a few nanometers thick) lies between the first medium (coverslip) and the high refractive index material (perovskite)[37]. In that work two-photon excitation was used, potentially resulting in a substantial EW penetration depth. One of the issues with this approach is that the air gap will vary in thickness (and therefore substantially in EW penetration) over the region of interest due to surface roughness of the substrate and the perovskite film, which will result in variations in any EWIF signal intensity. An alternative approach may be to use a thin film of a low refractive index material (e.g. a polymer) that can be cast with a uniform and controlled thickness. This was the motivation for the current work; the goal of this paper is to investigate the merit of this three-layer approach in terms of implementation in time-resolved EWIF measurements, and in a TIRF microscope to image, high refractive index materials in close proximity of a glass (or similar refractive index) substrate. A typical perovskite is used as a specific example of a high refractive index material for which this configuration may potentially be useful, and simulations are used to investigate the validity of this approach.

Simulation Details:

In this work we have performed simulations to analyze the behavior of the incident electromagnetic field for a simple, representative three-layer system consisting of silica (n_0 = 1.47),[38]† air (n_1 = 1.00),[39]† and a perovskite film (n_2 = 2.43)[40]. The wavelength of the incident EM beam is 400 nm. We have carried out these simulations using methods based on both a custom MATLAB script and the Finite Element Method as implemented in COMSOL Multiphysics. These two approaches are dealt with in the following two sections. Simulations were performed using MATLAB code based on the transfer matrix approach for calculation of the reflectance and transmittance of EM waves in a layered system.[41] Additional numerical methods-based simulations were performed using COMSOL Multiphysics® 5.5 with the Wave Optics Module. The geometry of the model is shown in Figure 2 with a modelled region of size 20 × 20 μm. An incident Gaussian beam with electric amplitude E_0

†COMSOL Multiphysics® 5.5 materials library

(Vm^{-1}) and beam width of 4 μm is applied to the left boundary of the cell. The thickness of the air layer and incident angle of the beam have been changed in the simulation to observe their effects attributed to the change of the electromagnetic field.

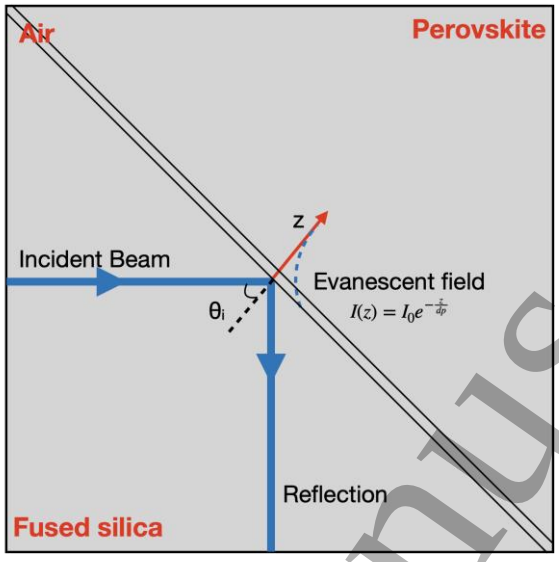

FIG. 2. Model geometry used for COMSOL simulations. Θ_i is the incident angle of the beam. z stands for the distance from silica-air interface. The generated evanescent field is expected to decay exponentially as a function of z.

Results and Discussion:

A model for a system with three media comprising silica, an air layer and a high refractive index material (perovskite) with an incident EM beam of 400 nm was developed as described above using the MATLAB-based analytical treatment. The light is incident through an optically thick silica TIR substrate (n_0), and the intensity of the incident EM wave reflected from the substrate:air interface is determined as a function of the angle of incidence (0 to 90°) and the thickness of air films (n_1, up to 1,000 nm). These simulations were performed for both *s*- and *p*-polarized incident light (Figure 3).

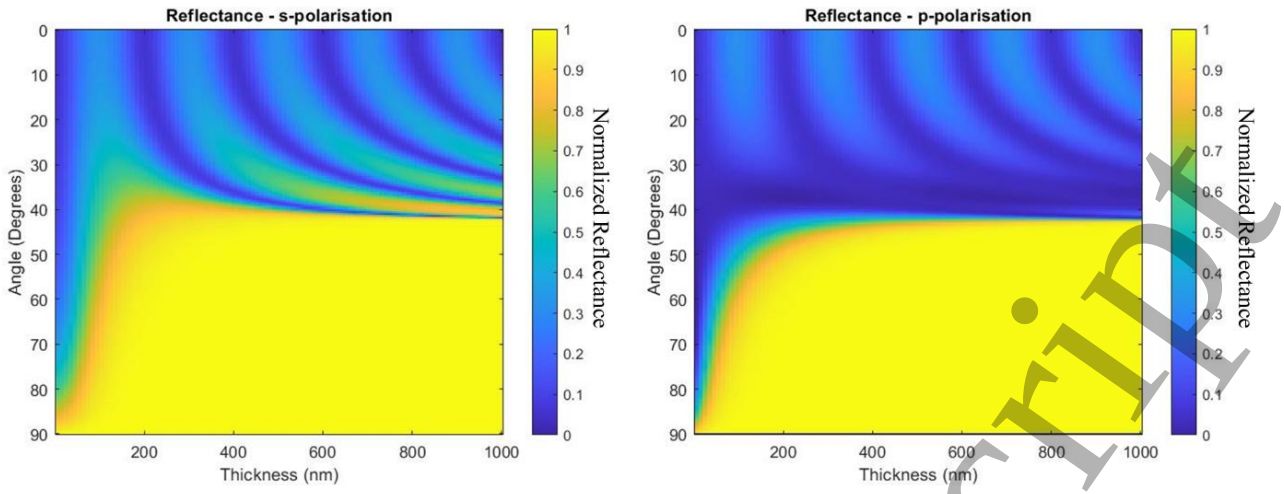

FIG. 3. Simulation of the reflectance of the incident radiation of wavelength 400 nm as a function of intermediate (air: n_1=1) film thickness and angle of incidence (n_0 (SiO_2) = 1.47, n_2 (perovskite) =2.43).

The critical angle for a silica-air interface is ~43° at 400 nm. From Figure 3, the reflectance of the system approaches unity after the incident angle exceeds the critical angle, corresponding to total internal reflection conditions. The behavior is similar for both the *s*- and *p*-polarization of the incident beam, for large intermediate layer thicknesses. At intermediate layer thicknesses, less than approximately 600 nm, the two polarization conditions exhibit different reflectance versus angle of incidence behavior. The reflectance from the interface as a function of angle of incidence at three representative intermediate layer thicknesses is shown in Figure 4.

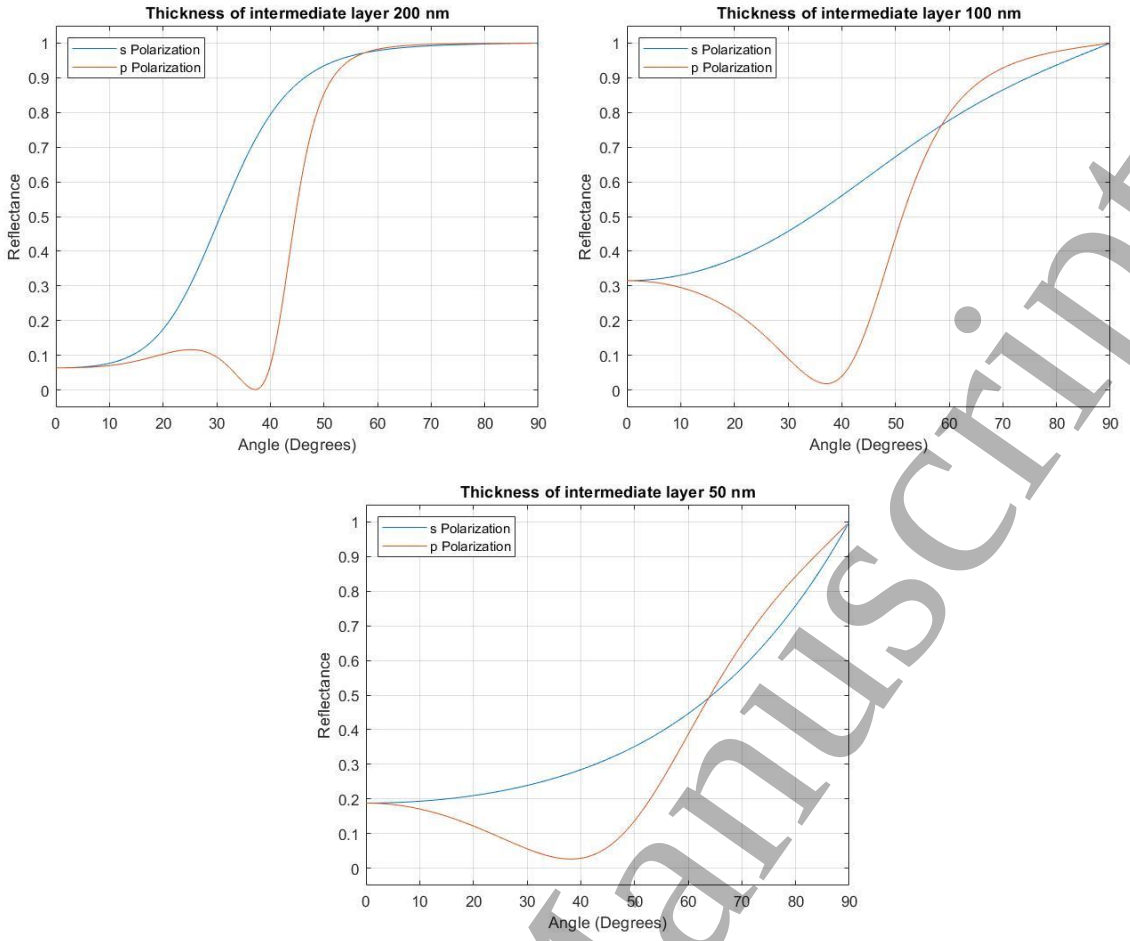

FIG. 4. Variation of the reflectance with the incidence angle for different thicknesses of the intermediate (air) layer.

The reflectance in all three cases exhibits a minimum value at around ~40° for *p*-polarized EM waves; around the Brewster angle for a glass: air interface. When the thickness of the intermediate layer is very small (50 nm or 100 nm), under *s*-polarized conditions, the reflectance of the system shows a gradual increase with increasing incidence angle. However, when the thickness of the intermediate layer is larger (e.g. 200 nm) the reflectance of the system under *s*-polarized conditions increases steeply with increasing angle of incidence up to the critical angle, after which the reflectance of the system tends to one (total internal reflection of the EM wave).

Therefore, we can conclude that a 400 nm EM wave incident on a Glass-Air-Perovskite system exhibits strong reflection at the glass air interface, for both polarization conditions, when the thickness of the intermediate air layer is greater than 200 nm, or about half the wavelength of the excitation light. If the thickness of the intermediate layer is below 200 nm the EM wave transmits directly from the glass

medium to the perovskite film and no or insignificant reflection of the incident wave exists. Therefore, no evanescent field is produced under these conditions and the advantages of interrogating the perovskite film using EW excitation (e.g. restricted penetration depth and polarization effects) cannot be exploited.

The thickness of the intermediate layer necessary for the strong reflection of the EM field has a strong dependence on the wavelength of the incident light. We have calculated the reflectance of the same system considering the wavelength of the incident EM wave to be 800 nm (Figure 5), typical of two photon-induced excitation as used in the papers of Doughty et al.[36,37] In this case the behavior is very similar to 400 nm excitation conditions; when the thickness of the intermediate (air) layer is very small the EM wave of 800 nm undergoes strong transmission from the first medium to the third medium experiencing frustrated total internal reflection. The incident EM field undergoes (near) total internal reflection beyond the critical angle only when the thickness of the middle layer is greater than $\lambda/2$ (~400 nm) where λ is the wavelength of the incident beam. This is expected as in the case where two angled prisms exhibiting TIR are brought close together - at a certain close separation the beam will transmit as the field couples from one prism into the other[5].

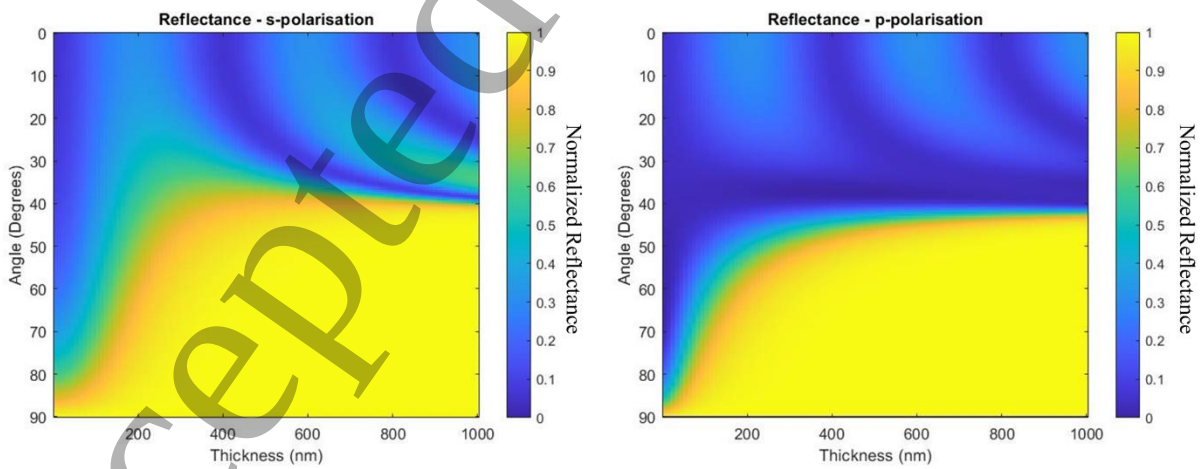

FIG. 5. Reflectance calculation of the incident EM wave of wavelength 800 nm as a function of intermediate (air: n_1=1) film thickness and angle of incidence (n_0 (SiO_2) = 1.47, n_2 (perovskite) =2.43)

As TIR of the incident EM field is a necessary condition for generating the evanescent wave at the interface of the first two layers, the intermediate layer must have a thickness of at least half the wavelength of the incident beam to generate an EW. However, if the distance over which the evanescent field decays is greater than the intermediate layer thickness, it may be plausible that the evanescent field could penetrate the third medium and excite the fluorophores for interrogating them by emission-based techniques affording the advantages of EW excitation.

For spectroscopically investigating the interfacial region of a perovskite film, under certain circumstances, the first medium may not need to possess a refractive index higher than the sample. Instead, it may be possible to find suitable combinations of the first medium and the intermediate layer and generate a decaying field in the third layer. There exist a few difficulties in the glass-air-perovskite configuration discussed above in optimizing the thickness of the intermediate air layer. The experimental arrangement of this system is quite difficult to establish while maintaining the desired thickness and uniformity of the air layer between the glass plate and the perovskite film. This problem could be overcome if the glass is coated with a thin film of a suitable low refractive index material and the sample is placed after the thin film. Therefore, instead of a glass-air-perovskite system we have also analyzed a glass-polymer film-perovskite system. It then remains to identify materials with the desired specific refractive indices to act as the intermediate film layer for the EWIF studies of high refractive index samples. Since the penetration depth of an evanescent field is a function of the relative refractive indices of the media constituting the interface, simulations can assist in identifying suitable material properties.

Similar MATLAB simulations to those performed for the silica-air-perovskite configuration were carried out on a glass-polymer film-perovskite system, calculating the reflectance as a function of the thickness of the intermediate film and angle of incidence, assuming 400 nm incident light (Figure 6). When the first medium (silica) is coated with the (polymer) film with a refractive index of 1.35, the critical angle of the silica-film interface is around ~ 66°, after which the system exhibits TIR. The

reflectance of the system is minimum for an incident *p*-polarized wave around an incident angle ~ 42°, which corresponds to the Brewster angle for the glass-film interface. The thickness of the intermediate layer also plays a critical role in the behavior of the incident electromagnetic field at the interface. The reflectance of the system is not very strong even after the critical angle when the thickness of the intermediate layer is below 200 nm. Consequently, the EM wave does not reflect totally from the interface, but it directly transmits to the third medium, i.e. into the perovskite film. We have earlier seen the similar effects with the glass-air interface.

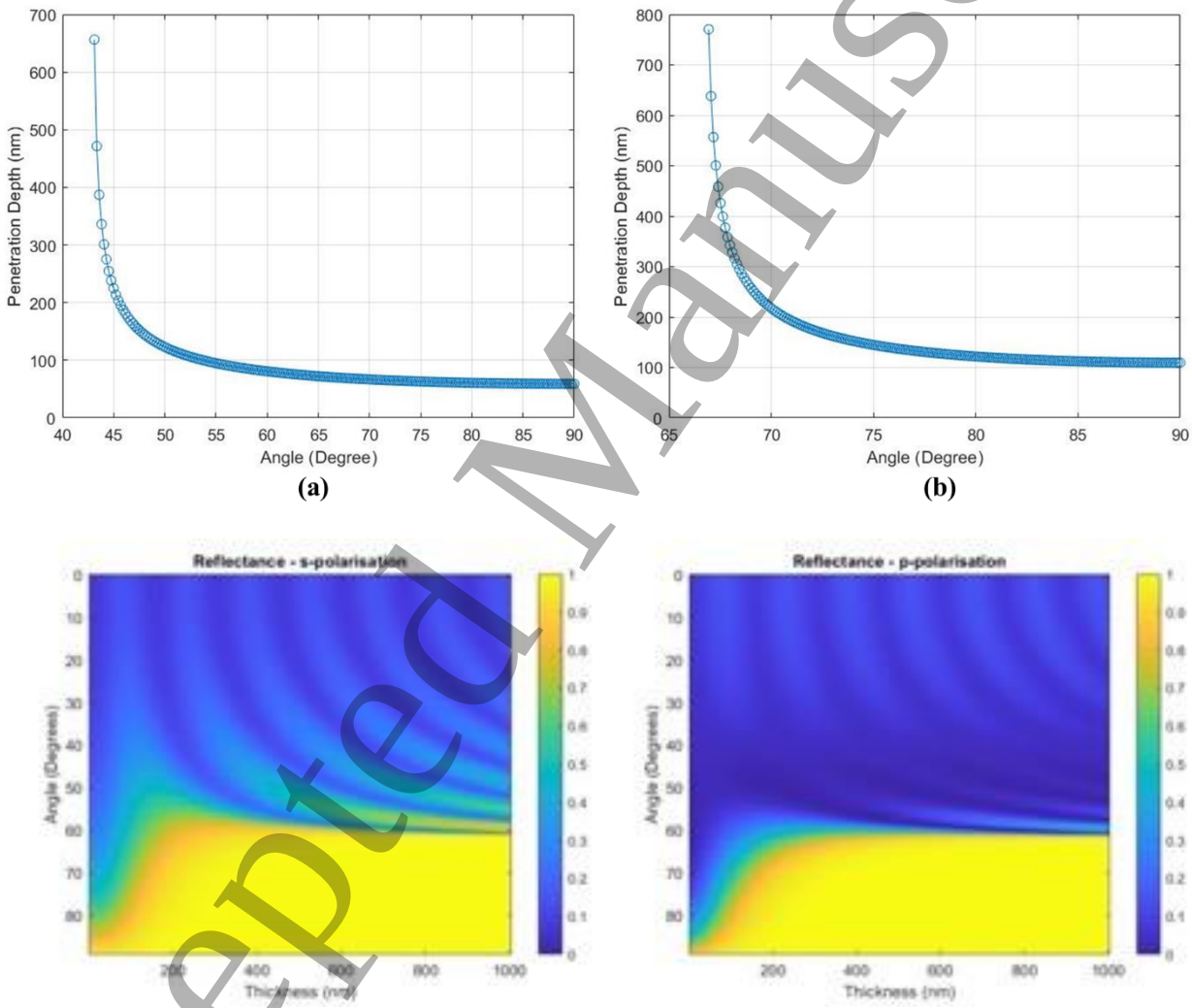

FIG. 6. Variation of the penetration depth of the evanescent field for (a) the silica- air interface and (b) the silica-polymer film interface. Reflectance calculation of the incident EM wave (400 nm) in a glass-film-perovskite configuration ($n_1 = 1.35$).

Considering that TIR is only viable when the thickness of the n_1 film is approximately half the wavelength of the incident light, in this case, a penetration depth in medium 1 of at least 200 nm is required. For the evanescent field to be of sufficient strength at the n_1:n_2 interface to probe

fluorophores in the n_2 material the penetration depth needs to be significantly larger than this. Figure 6 represents the variation in the penetration depth of the evanescent field as a function of the incident angle for the two configurations discussed above. The penetration depth is undefined (infinite) at the critical angle (Equation 1) but is very strongly dependent on the angle of incidence for angles just larger than the critical angle. For s silica-air interface the critical angle after which the TIR is exhibited is ~ 42.86°. The penetration depth, in this case, falls below 200 nm if the angle of incidence is increased from θ_c by more than just a few degrees in this case. The critical angle for the silica-film interface is ~ 66.68° and in this case, the penetration depth falls below 200 nm when the angle of incidence exceeds 70 degrees. Therefore, for interrogating the high refractive index perovskite films via evanescent wave excitation at 400 nm, a silica-polymer film-perovskite configuration with a polymer film thickness of ~200 nm and an incidence angle just beyond the critical angle *may* appear to be a viable arrangement.

The numeric simulations above lead to the optimal parameters of the various layers, but do not interrogate the penetration of the evanescent wave produced at the n_0:n_1 interface into the n_2 material. For this, we have performed numerical-based simulations using COMSOL Multiphysics. In the first of these simulations, we investigated the effects induced by the intermediate layer on evanescent field generation, as the thickness of the intermediate layer (t_{air}) was varied from 10 nm to 390 nm at a constant angle of incidence (45^o - just larger than the critical angle) and the corresponding electric field distributions compared (Figure 7). The intensity of the reflected beam decreases with decreasing t_{air}, i.e. as the silica and perovskite layers become closer. This is in agreement with the MATLAB simulations and supports the viability of the proposed 3-layer approach. Moreover, the electric field plots (Figure 7(c)) show a discontinuity after reaching the perovskite layer, however, the field strength does decay with increasing distance from the interface, albeit with a different distance dependence beyond the point of the discontinuity.

(a)

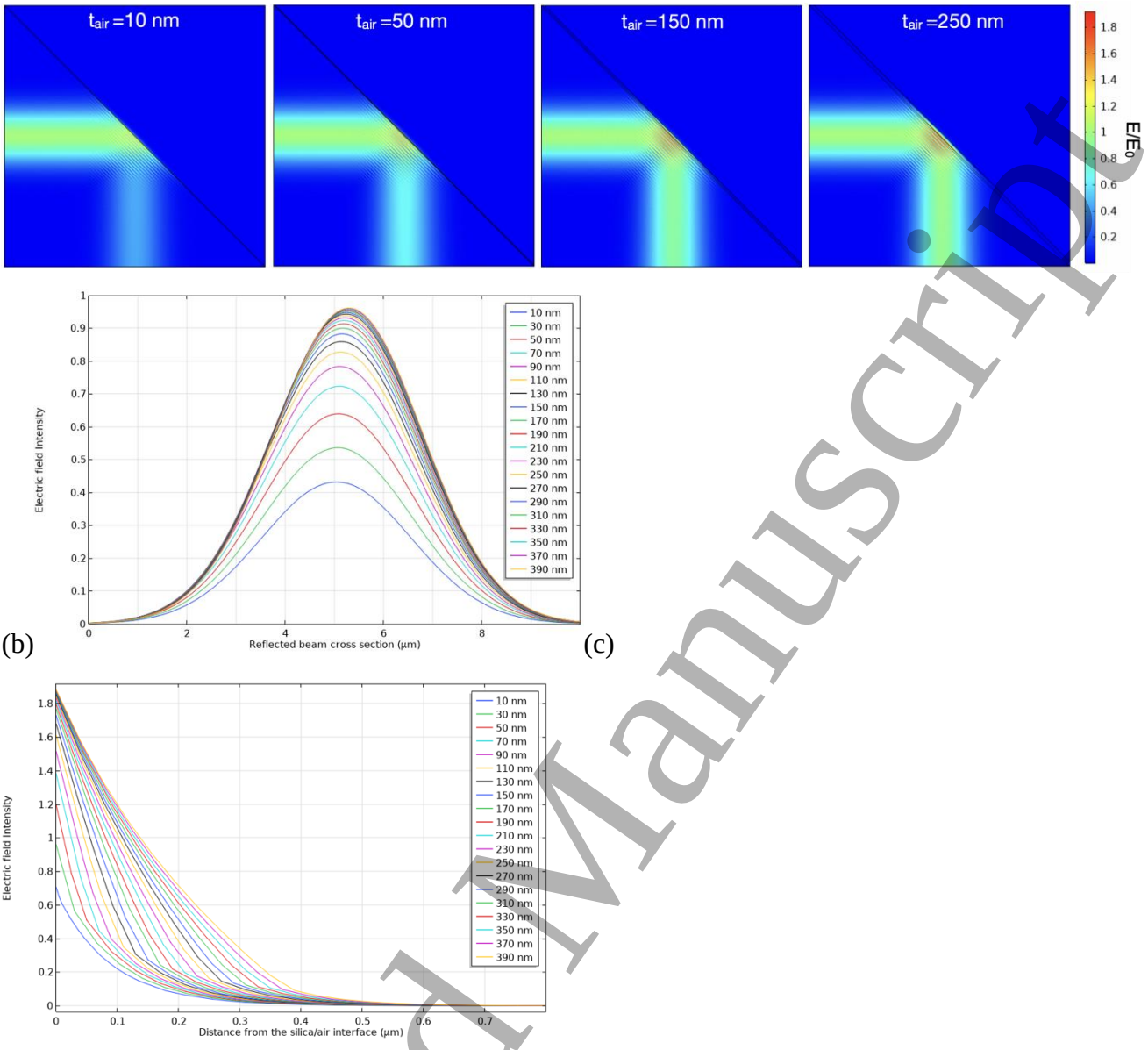

(b) (c)

FIG. 7. COMSOL simulation results that are based on silica-air-perovskite multilayer structures under various thicknesses of the intermediate layer (t_{air}). (a) Electric field distributions in the system. (b) Plots of the intensity of the reflected beam; (c) Plots of field intensity as a function of distance from the silica/air interface. The incident electric field is set to be s-polarized. Incident wavelength = 400nm. Incident angle = 45°.

To further examine the discontinuity and field decay, another simulation was run in which the absorption of the perovskite (the imaginary component of the refractive index, $n = (n + i\kappa)$, where κ is the extinction coefficient, and the absorption coefficient, $\alpha = 4\pi\kappa/\lambda$) is not considered. The extinction coefficient of the perovskite layer was set to 0, while all the other parameters were the same as above. Figure 8 shows the electric field is surprisingly different from Figure 7 above. Although the evanescent field can be seen in the air layer, its field intensity remains constant after reaching the perovskite layer,

which again indicates that when the EW generated at the second layer reaches the third layer, it exists as a propagating wave rather than as an EW.

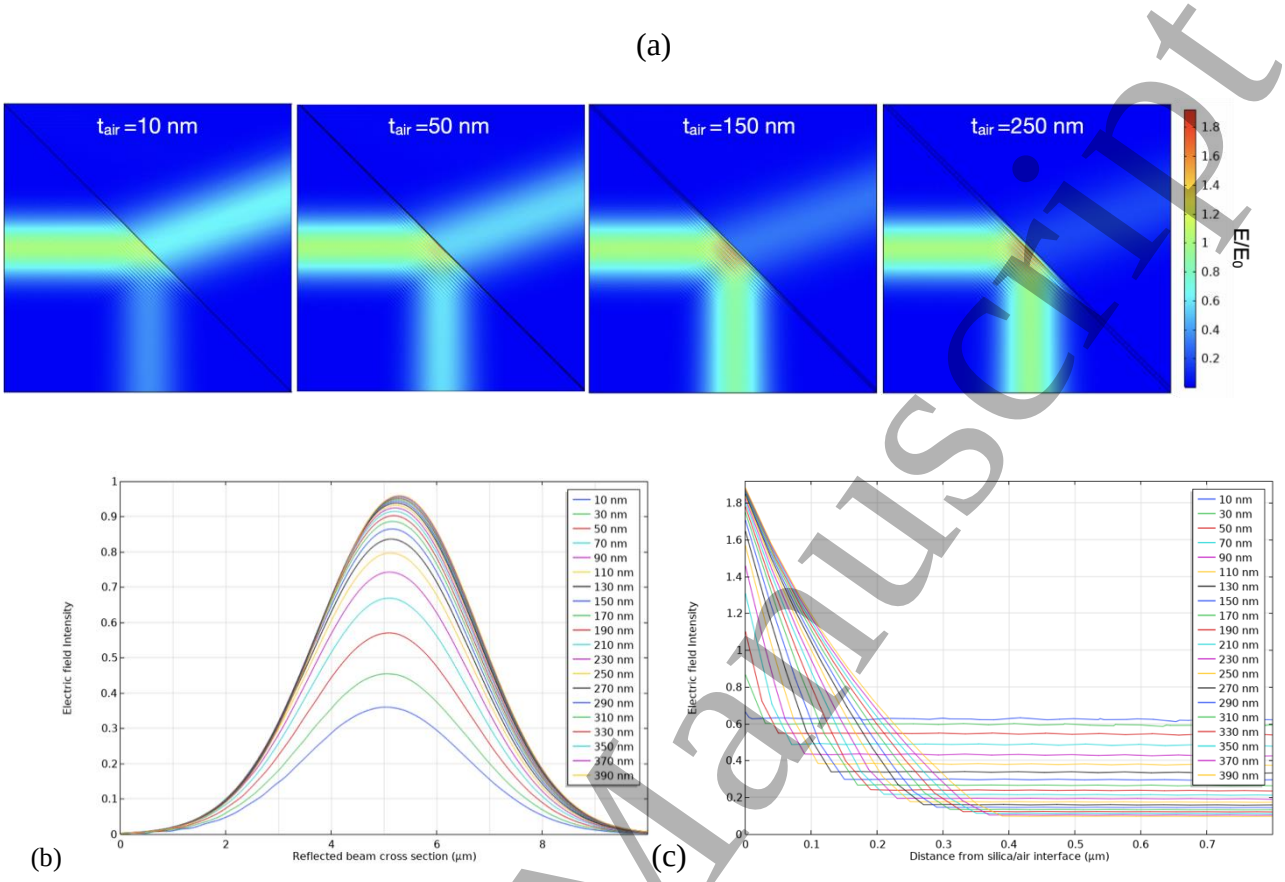

FIG. 8. COMSOL simulation results based on silica-air-perovskite multilayer structures under various thickness of intermediate layer (t_{air}), with absorption of perovskite layer NOT considered. (a) Electric field distributions in the system. (b) Plots of the intensity of reflected beam; (c) Plots of field intensity as a function of distance from the silica-air interface. Incident electric field is set to be *s*-polarized. Incident wavelength = 400nm. Incident angle=45°.

Conclusions:

In conclusion, a multilayer approach to using evanescent wave excitation is explored through simulations using both MATLAB and COMSOL code. The MATLAB code predicts that this approach may be viable under certain conditions (wavelength and intermediate layer thickness) for probing the interfacial behavior of high refractive index materials.[36,37] However, the COMSOL simulations illustrate that, in the three-layer system we modeled here, the evanescent field only exists in the intermediate (low refractive index) layer, decaying exponentially, but then behaves as a propagating wave after reaching the high refractive index (e.g. perovskite) layer exhibiting frustrated total internal reflection. Theses simulations, therefore, show that the three-layer approach is not viable for probing

high refractive index materials exploiting the advantages of EWIF spectroscopy, specifically its two key capabilities; (i) to probe emission as a function of distance from the interface (through variable angle excitation) and (ii) to preferentially excite absorption transition dipoles oriented parallel and perpendicular to the interface, cannot, therefore, be exploited with this simple three-layer configuration. This work suggests that the assumption made in previous work[36,37] in terms of the penetration of the EW into the high refractive index material is not valid, and alternative methods of probing materials such as perovskites must be employed.

Ethical Compliance:

There are no ethical compliance issues related to this manuscript.

Data Access Statement:

Research data supporting this publication are available directly from the authors.

Conflict of Interest Statement

The authors have no conflicts of interest to declare.

References

[1] Schneckenburger H. Total internal reflection fluorescence microscopy: Technical innovations and novel applications. In *Current opinion in biotechnology*, 2005.
[2] Simpson T R E, Revell D J, Cook M J and Russell D A 1997 Evanescent wave excited fluorescence from self-assembled phthalocyanine monolayers *Langmuir* **13**, 460.
[3] Woerdeman D L, Flynn K M, Dunkers J P and Parnas R S 1996 The use of evanescent wave fluorescence spectroscopy for control of the liquid molding process *Journal of Reinforced Plastics and Composites* **15**, 922.
[4] Hecht E *Optics*, 5th ed.; Pearson Education India, 2002.
[5] Harrick N J *Internal reflection spectroscopy*; John Wiley & Sons, Wiley-Inter-Science Div.: New York, 1967.
[6] Neivandt D and Gee M L 1995 Variable angle of incidence evanescent wave spectroscopy of the adsorption of quaternarized poly(vinylpyridine) on silica *Langmuir* **11**, 1291.
[7] Rumbles G, Brown A J, Phillips D and Bloor D 1992 Surface-induced chromism and enhanced fluorescence of the soluble polydiacetylene, poly(4=butoxycarbonylmethylurethane), at a solid/solution interface: An evanescent-wave induced fluorescence study *J. Chem. Soc. Faraday Trans.* **88**, 3313.

[8] Axelrod D. Total internal reflection fluorescence microscopy. In *Encyclopedia of cell biology*, 2016.
[9] Poulter N S, Pitkeathly W T E, Smith P J and Rappoport J Z. The physical basis of total internal reflection fluorescence (TIRF) microscopy and its cellular applications. In *Advanced fluorescence microscopy: Methods and protocols*; P.J. Verveer, Ed.; Springer New York: New York, NY, 2015; pp 1.
[10] Kudalkar E M, Davis T N and Asbury C L 2016 Single-molecule total internal reflection fluorescence microscopy *Cold Spring Harb Protoc* **2016**, pdb.top077800.
[11] Rego E H, Shao L, Macklin J J, Winoto L, Johansson G A, Kamps-Hughes N, Davidson M W and Gustafsson M G L 2012 Nonlinear structured-illumination microscopy with a photoswitchable protein reveals cellular structures at 50-nm resolution *Proceedings of the National Academy of Sciences* **109**, E135.
[12] Roth J, Mehl J and Rohrbach A 2020 Fast TIRF-SIM imaging of dynamic, low-fluorescent biological samples *Biomedical Optics Express* **11**, 4008.
[13] Rumbles G, Bloor D, Brown A J, Crystall B, Phillips D and Smith T A. Time-resolved evanescent wave-induced fluorescence studies of polymer-surface interactions. In *Microchemistry. Spectroscopy and chemistry in small domains*; H. Masuhara, Ed.; North-Holland, 1994; pp 269.
[14] Smith T A, Scholes C A and Gee M L. Time-resolved evanescent wave-induced fluorescence studies of macromolecular adsorption. In *Proc. of SPIE: Complex Light and Optical Forces*; D.L. Andrews, E.J. Galvez, G. Nienhuis, Eds.; Proc. SPIE, 2007; Vol. 6483; pp 64830C1.
[15] Ishizaka S, Kim H-B and Kitamura N 2001 Time-resolved total internal reflection fluorometry study on polarity at a liquid/liquid interface *Analytical Chemistry* **73**, 2421.
[16] Delgado H E, Rumbach P, Bartels D M and Go D B 2018 Total internal reflection absorption spectroscopy (tiras) for the detection of solvated electrons at a plasma-liquid interface *JoVE*, e56833.
[17] Kabardin I K, Meledin V G, Eliseev I A and Rakhmanov V V 2011 Optical measurement of instantaneous liquid film thickness based on total internal reflection *Journal of Engineering Thermophysics* **20**, 407.
[18] SiO_2 refractive index. https://refractiveindex.info/?shelf=main&book=SiO2&page=Malitson.
[19] Al_2O_3 refractive index. https://refractiveindex.info/?shelf=main&book=Al2O3&page=Malitson-o.
[20] Morikawa T, Shirai E, Tanno J, Takanashi H, Yasuda A and Itoh K 1998 Time-resolved total internal reflection raman scattering study on electric-field-induced reorientation dynamics of nematic liquid crystal of 4-hexyl-4'-cyanobiphenyl *Mol. Cryst. Liq. Cryst.* **312**, 69.
[21] Ohara Inc. $LaSFO_8$ refractive index. Refractive index of hikari - lasf ($lasfo_8$); https://www.ohara-inc.co.jp/assets/en/product/pdf/eslah58.pdf, https://refractiveindex.info/?shelf=glass&book=HIKARI-LaSF&page=J-LASF08.
[22] Starr T E and Thompson N L 2000 Formation and characterization of planar phospholipid bilayers supported on tio_2 and $SrTiO_3$ single crystals *Langmuir* **16**, 10301.
[23] TiO_2 refractive index. https://refractiveindex.info/?shelf=main&book=TiO2&page=Devore-o.
[24] $SrTiO_3$ refractive index. https://refractiveindex.info/?shelf=main&book=SrTiO3&page=Dodge.
[25] Salomon L, De Fornel F and Goudonnet J P 1991 Sample–tip coupling efficiencies of the photon-scanning tunneling microscope. *JOSA A.* **8**, 2009.
[26] Shirota M, van Limbeek M A, Lohse D and Sun C 2017 Measuring thin films using quantitative frustrated total internal reflection (FTIR) *European Physical J. E* **40**, 1.
[27] Plenet J C, Othmani A, Paille F, Mugnier J, Bernstein E and Dumas J 1997 Linear optical properties of high concentration silica CdS doped thin films elaborated by sol-gel route *Optical Materials* **7**, 129.

[28] Kaiser R, Lévy Y, Vansteenkiste N, Aspect A, Seifert W, Leipold D and Mlynek J 1994 Resonant enhancement of evanescent waves with a thin dielectric waveguide *Opt. Comm.* **104**, 234.
[29] Hassanzadeh A and Azami D 2015 Graphene based resonance structure to enhance the optical pressure between two planar surfaces *Opt Express* **23**, 33681.
[30] Darya Azami, Abdulkareem S S and Hassanzadeh A Resonant enhancement of evanescent waves with graphene and double-negative materials in the visible regime *Journal of Nanophotonics* **14**, 036003/1.
[31] Sadrolhosseini A R, Shafie S and Fen Y W 2019 Nanoplasmonic sensor based on surface plasmon-coupled emission: Review *Applied Sciences* **9**, 1497.
[32] Gryczynski Z, Gryczynski I, Matveeva E, Malicka J, Nowaczyk K and Lakowicz J R. Surface-plasmon–coupled emission: New technology for studying molecular processes. In *Methods in cell biology*; Academic Press, 2004; Vol. 75; pp 73.
[33] Jiang Y, Pillai S and Green M A 2016 Realistic silver optical constants for plasmonics *Scientific Reports* **6**, 30605.
[34] Ag refractive index. https://refractiveindex.info/?shelf=main&book=Ag&page=Johnson.
[35] Ray K, Szmacinski H, Enderlein J and Lakowicz J R 2007 Distance dependence of surface plasmon-coupled emission observed using Langmuir-Blodgett films *Applied Physics Letters* **90**, 251116.
[36] Watson B R, Yang B, Xiao K, Ma Y-Z, Doughty B and Calhoun T R 2015 Elucidation of perovskite film micro-orientations using two-photon total internal reflectance fluorescence microscopy *J. Phys. Chem. Lett.* **6**, 3283−3288.
[37] Liu Y, Collins L, Proksch R, Kim S, Watson B R, Doughty B, Calhoun T R, Ahmadi M, Ievlev A V, Jesse S, Retterer S T, Belianinov A, Xiao K, Huang J, Sumpter B G, Kalinin S V, Hu B and Ovchinnikova O S 2018 Chemical nature of ferroelastic twin domains in $CH_3NH_3PbI_3$ perovskite *Nature Materials* **17**, 1013.
[38] Malitson I H 1965 Interspecimen comparison of the refractive index of fused silica, *Journal of the Optical Society of America* **55**, 1205.
[39] Ciddor P E 1996 Refractive index of air: New equations for the visible and near infrared *Applied Optics* **35**, 1566.
[40] Phillips L J, Rashed A M, Treharne R E, Kay J, Yates P, Mitrovic I Z, Weerakkody A, Hall S and Durose K 2015 Dispersion relation data for methylammonium lead triiodide perovskite deposited on a (100) silicon wafer using a two-step vapour-phase reaction process *Data Brief.* **Nov 6;5**, 926.
[41] Macleod H A *Thin-film optical filters*, 5th ed.; Routledge: Boca Raton, 2017.